

See discussions, stats, and author profiles for this publication at: <https://www.researchgate.net/publication/263985004>

Dry Deposition of Biogenic Terpenes via Cationic Oligomerization on Environmental Aqueous Surfaces

ARTICLE *in* JOURNAL OF PHYSICAL CHEMISTRY LETTERS · OCTOBER 2012

Impact Factor: 7.46 · DOI: 10.1021/jz301294q

CITATIONS

14

READS

14

3 AUTHORS, INCLUDING:



Michael R. Hoffmann

California Institute of Technology

408 PUBLICATIONS 30,268 CITATIONS

SEE PROFILE



Agustin J Colussi

California Institute of Technology

233 PUBLICATIONS 4,304 CITATIONS

SEE PROFILE

Dry Deposition of Biogenic Terpenes via Cationic Oligomerization on Environmental Aqueous Surfaces

Shinichi Enami*

The Hakubi Center for Advanced Research, Kyoto University, Kyoto 606-8302, Japan, Research Institute for Sustainable Humanosphere, Kyoto University, Uji 611-0011, Japan, and PRESTO, Japan Science and Technology Agency, Kawaguchi 332-0012, Japan

Michael R. Hoffmann and Agustín J. Colussi*

Ronald and Maxine Linde Center for Global Environmental Science, California Institute of Technology, California 91125, United States

S Supporting Information

ABSTRACT: Unraveling the complex interactions between the atmosphere and the biosphere is critical for predicting climate changes. Although it is well-recognized that the large amounts of biogenic volatile organic compounds (BVOCs) emitted by plants must play important roles in this regard, current atmospheric models fail to account for their fate due to missing chemical sinks. Here, we applied online electrospray mass spectrometry to monitor aqueous microjets exposed to gaseous monoterpenes (α -pinene, β -pinene, and d -limonene) and found that these BVOCs are readily protonated (to $C_{10}H_{17}^+$) and undergo oligomerization (to $C_{20}H_{33}^+$ and $C_{30}H_{49}^+$) upon colliding with the surface of pH < 4 microjets. By considering that the yields of all products show inflection points at pH \approx 3.5 and display solvent kinetic hydrogen isotope effects larger than 2, we conclude that the oligomerization process is initiated by weakly hydrated hydronium ions, H_3O^+ , present at the gas–water interface. Present results provide a universal mechanism for the dry deposition of unsaturated BVOCs and may account for recent observations on the uptake of terpenes in forest canopies and over grassland.



SECTION: Environmental and Atmospheric Chemistry, Aerosol Processes, Geochemistry, and Astrochemistry

It is estimated that ~ 630 Tg C/year of gaseous unsaturated hydrocarbons are emitted to the atmosphere, about half of which are biogenic volatile organic compounds (BVOCs).^{1–3} Despite the magnitude of these numbers and the anticipated response of this global process to anthropogenic perturbations, it is still unclear how they are removed from the atmosphere and what fraction it is converted to atmospheric aerosols.^{4,5} In the past, BVOCs were deemed to be largely processed in the gas phase by reacting with atmospheric oxidants such as ozone and OH radicals, followed by condensation of the resulting products into aerosol particles.^{6,7} Laboratory and field studies and model calculations, however, have revealed the need for additional sinks involving the direct uptake of BVOCs, which remain to be characterized.^{8,9} There is now clear evidence of the direct uptake of BVOCs in forest canopies and over grassland fields,^{10,11} that is, in settings that, by providing large surface-to-volume ratios and relatively long gas–surface contact times, favor heterogeneous processes. Remarkably, the reported BVOCs deposition rates in both scenarios approach the aerodynamic limit,^{10,11} that is, they are controlled by an uptake process that operates with high efficiency during gas–surface collisions.^{12,13}

We recently found in the laboratory that isoprene, ISO, the primordial biogenic gas, is protonated on pH < 4 aqueous

surfaces and presented evidence that such acidities may be prevalent in the aqueous films lining the surfaces of leaves, soil, and aerosol particles.¹² We also advanced the notion that this unforeseen phenomenon is triggered by the superacidity of weakly hydrated hydronium ions H_3O^+ at the air–water interface.^{14,15} In this connection, we point out that gaseous H_3O^+ can protonate most unsaturated hydrocarbons, as attested by the versatility of proton-transfer reaction mass spectrometry (PTR-MS),¹⁶ but its superacidity is gradually lost upon increasing hydration.¹⁵ Although there is experimental evidence that α -pinene polymerizes on highly acidic (pH < 0) aerosols in chamber experiments,¹⁷ the idea that such a process could also take place on less acidic, more representative environmental aqueous surfaces appears to have been overlooked. Herein, we aim at characterizing the mechanism of a general uptake process in which the irreversible incorporation of unsaturated BVOCs onto representative wet environmental surfaces is not controlled by postcollisional events.

Our experiments are conducted by intersecting continuously refreshed, uncontaminated surfaces of free-flowing aqueous

Received: August 29, 2012

Accepted: October 8, 2012

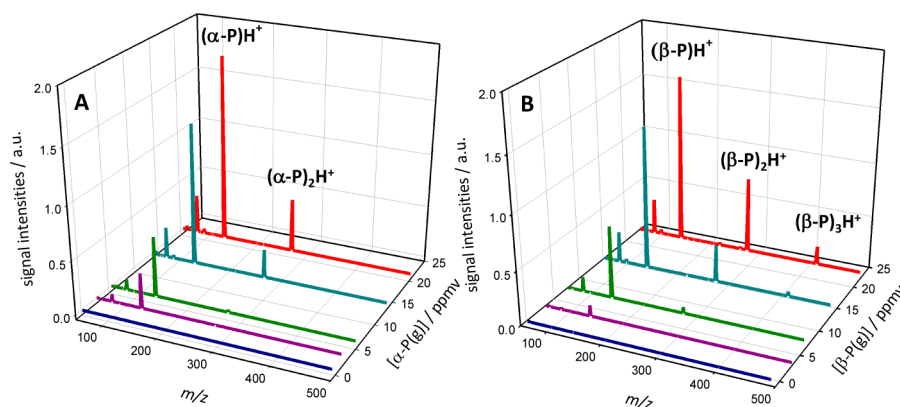


Figure 1. Positive ion ES mass spectra of pH 2.6 water microjets exposed to various $[\alpha\text{-P(g)}]$ (A) or $[\beta\text{-P(g)}]$ for $\tau \approx 10\text{--}50\ \mu\text{s}$; $1\ \text{ppmv} = 2.4 \times 10^{13}\ \text{molecules cm}^{-3}$ at 1 atm and 298 K experimental conditions. The $m/z = 81$ (C_6H_9^+) is a fragment of $m/z = 137$ ($\text{C}_{10}\text{H}_{17}^+$).

microjets with a gaseous terpene (α -pinene (α -P), β -pinene (β -P), or d -limonene (d -L)) beam and detecting the formation of interfacial cations by online electrospray mass spectrometry (ES-MS)¹⁸ (see the Experimental Section, the Supporting Information (SI), and Figure S1). Figure 1 shows positive ion ES mass spectra of the surface of water microjets at pH 2.6 exposed to $\alpha\text{-P(g)}/\text{N}_2\text{(g)}$ or $\beta\text{-P(g)}/\text{N}_2\text{(g)}$ mixtures for $\sim 10\text{--}50\ \mu\text{s}$. Throughout, pH is the pH of the injected solutions, adjusted with HCl and measured with a calibrated pH meter prior to injection. Gas–liquid contact times correspond to the lifetimes of the intact microjets before they are broken up by the nebulizer gas into charged microdroplets carrying the information (in the form of excess charge) acquired by the mass spectrometer.¹⁸ Note the intense ES mass spectral signals at $m/z = 81$, 137 ($\text{C}_{10}\text{H}_{16} + \text{H}^+$), and 273 ($2\ \text{C}_{10}\text{H}_{16} + \text{H}^+$) Da. A similar product's mass spectrum was observed from the exposure to $d\text{-L(g)}$. A product of 409 ($3\ \text{C}_{10}\text{H}_{16} + \text{H}^+$) Da was observed only for β -P above a few ppmv but was absent in experiments involving α -P or d -L up to 95 and 40 ppmv, respectively. We did not find products of mass > 500 Da under any conditions. These terpenes, whose gas-phase proton affinities ($\text{PA} \approx 220\ \text{kcal mol}^{-1}$) are much larger than that of water ($\text{PA} = 165\ \text{kcal mol}^{-1}$),¹⁹ are readily protonated in interfacial layers, giving rise to the corresponding carbocations. The $m/z = 81$ and 95 signals are assigned to the known fragments of the collisionally induced decomposition of protonated monoterpenes $\text{C}_{10}\text{H}_{17}^+$ ($m/z = 137$) into C_6H_9^+ ($+ \text{C}_4\text{H}_8$) and $\text{C}_7\text{H}_{11}^+$ ($+ \text{C}_3\text{H}_6$), respectively,²⁰ in accord with the reciprocal evolution of $m/z = 81$ and 95 versus $m/z = 137$ and 273 signal intensities as functions of the fragmentation voltage (see Figure S2, SI). Note that only β -P gives rise to a trimer, $\text{C}_{30}\text{H}_{49}^+$, whereas α -P and d -L stop at the dimers $\text{C}_{20}\text{H}_{33}^+$ under similar conditions.¹⁷ Because all primary carbocations $\text{C}_{10}\text{H}_{17}^+$ probably undergo rapid isomerization into a common set of propagating intermediates via intramolecular proton transfers and/or structural rearrangements, the implication is that the exo double bond of β -P is a better nucleophile than the ring or vinyl double bonds of α -P and d -L.^{21,22} Alternatively, the dimer $\text{C}_{30}\text{H}_{49}^+$ carbocations of α -P and d -L could react faster than β -P with water, thereby terminating polymerization.²³

The absence of any protonated product signals in the ES mass spectra of 1 mM α -P in water/acetonitrile (50/50 = vol/vol) solutions at $1.1 < \text{pH} < 6.0$ or in water/methanol (50/50) solutions at $1.5 < \text{pH} < 7.5$ demonstrates that α -P is protonated at the gas side rather than the bulk side of the interface.¹⁵ It also

proves that the carbocations detected in these experiments are indeed produced at the gas–liquid interface, in accordance with the evidence obtained in previous experiments.^{9,18,24–26}

Figure 2A shows that both $(\alpha\text{-P})\text{H}^+$ and $(\alpha\text{-P})_2\text{H}^+$ products appear only below $\text{pH} \approx 4$ and evolve along a common titration curve possessing an inflection point at $\text{pK}_a = 3.54 \pm 0.26$. Note that the yields of these products are negligible at $\text{pH} = 7$, confirming that hydronium (or a proton) is needed for their

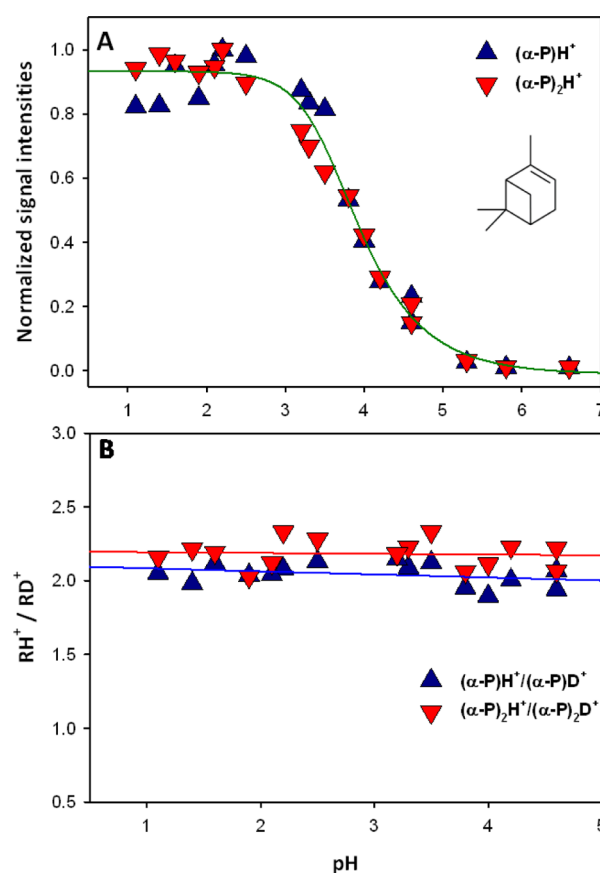


Figure 2. (A) Normalized $(\alpha\text{-P})\text{H}^+$ ($m/z = 137$) and $(\alpha\text{-P})_2\text{H}^+$ ($m/z = 273$) ES mass spectral signal intensities. (B) Ratios of $M/(M+1)$ ES mass spectral signal intensities as a function of bulk pH, in experiments performed on $\text{H}_2\text{O}/\text{D}_2\text{O}$ (50/50 = vol/vol) microjets exposed to 27.3 ppmv $\alpha\text{-P(g)}$ for $\tau \approx 10\text{--}50\ \mu\text{s}$ contact times. All experiments are in 1 atm of $\text{N}_2\text{(g)}$ at 298 K.

formation. The experimental titration curves for β -P and d -L are very similar, having inflection points at $pK_a = 3.51 \pm 0.40$ (Figure 3A) and 3.63 ± 0.05 (Figure 4A), respectively. These

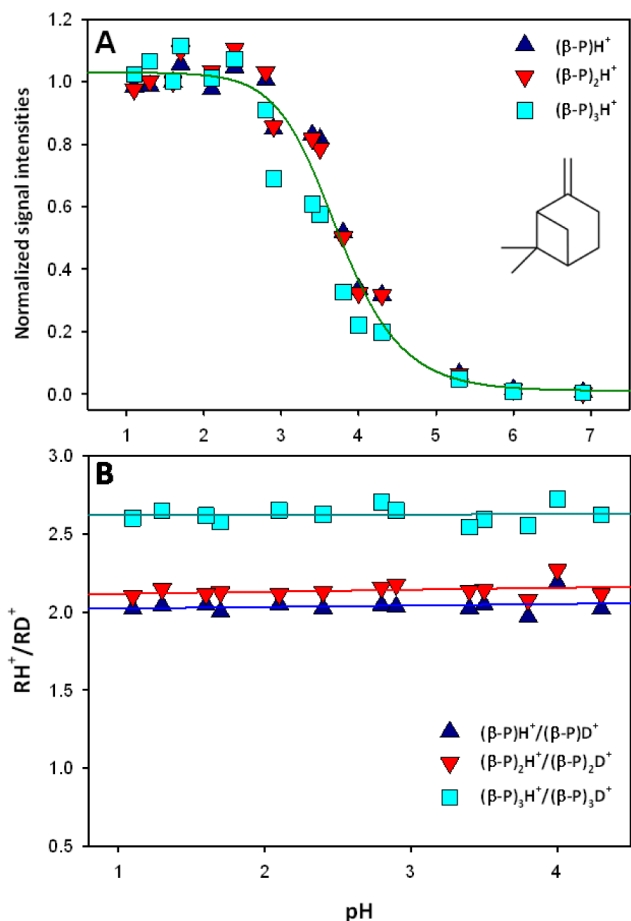


Figure 3. (A) Normalized $(\beta\text{-P})\text{H}^+$ ($m/z = 137$), $(\beta\text{-P})_2\text{H}^+$ ($m/z = 273$), and $(\beta\text{-P})_3\text{H}^+$ ($m/z = 409$) ES mass spectral signal intensities. (B) Ratios of $M/(M+1)$ ES mass spectral signal intensities as a function of bulk pH, in experiments performed on $\text{H}_2\text{O}/\text{D}_2\text{O}$ (50/50 = vol/vol) microjets exposed to 30.7 ppmv $\beta\text{-P}(\text{g})$ for $\tau \approx 10\text{--}50 \mu\text{s}$ contact times. All experiments are in 1 atm of $\text{N}_2(\text{g})$ at 298 K.

results clearly confirm our previous reports on the emergence of strongly acidic hydronium species, $\text{H}_3\text{O}^+(\text{if})$, to the surface of $\text{pH} \leq 4$ water,^{15,18} that is, the coincidental titration curves found for the three monoterpenes reflect a property of the surface of water rather than that of the proton acceptors. $\text{H}_3\text{O}^+(\text{if})$ behaves as a partially hydrated species that, like $\text{H}_3\text{O}^+(\text{g})$, can protonate gases having proton affinities larger than that of gaseous water ($\text{PA} = 165 \text{ kcal mol}^{-1}$).¹⁹ Significantly, most BVOCs meet such a requirement and would be similarly protonated on the surface of mildly acidic water.¹⁹ Because the $pK_a \approx 3.5$ derived from Figures 2A, 3A, and 4A nearly matches the $pK_a \approx 3$ previously measured in experiments using the much weaker base hexanoic acid gas ($\text{PA} = 187 \text{ kcal mol}^{-1}$) as the proton acceptor,¹⁵ we infer that the titration curves reflect an equilibrium established “on water” rather than in the gas phase. A common titration curve for all signals further implies that the protonation of terpenes is the rate-determining step, that is, that the rate constants for

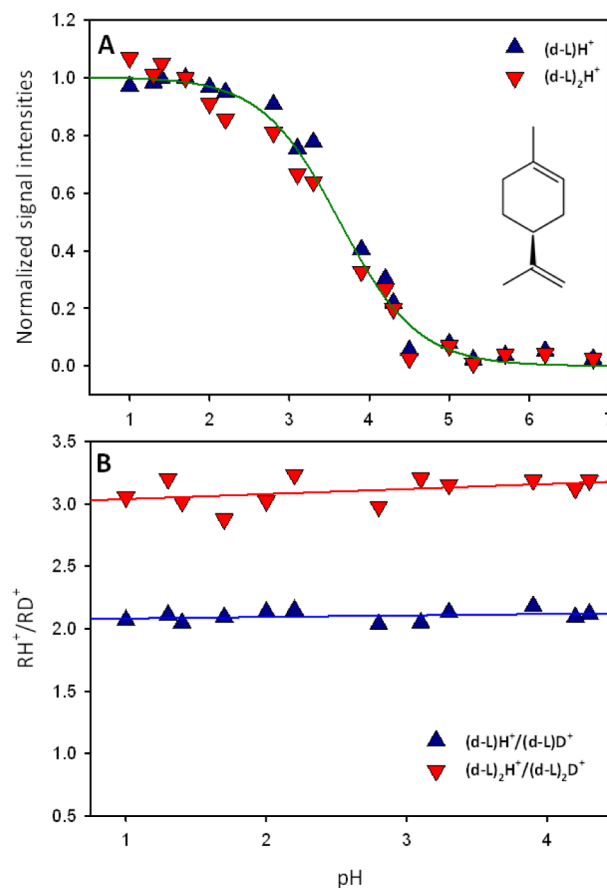
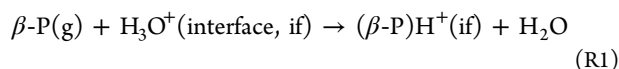
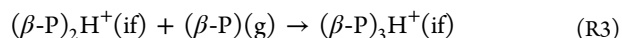
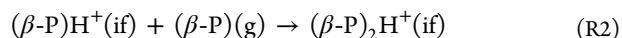


Figure 4. (A) Normalized $(d\text{-L})\text{H}^+$ ($m/z = 137$) and $(d\text{-L})_2\text{H}^+$ ($m/z = 273$) ES mass spectral signal intensities. (B) Ratios of $M/(M+1)$ ES mass spectral signal intensities as a function of bulk pH, in experiments performed on $\text{H}_2\text{O}/\text{D}_2\text{O}$ (50/50 = vol/vol) microjets exposed to 20.3 ppmv $d\text{-L}(\text{g})$ for $\tau \approx 10\text{--}50 \mu\text{s}$ contact times. All experiments are in 1 atm of $\text{N}_2(\text{g})$ at 298 K.



are in the order $k_1 < k_2 \approx k_3$. The observation that the cationic oligomerization proceeds even in the presence of water (a strong base known to quench cationic polymerization in bulk liquids even at trace levels) is striking evidence of the low activity of water at the gas–liquid interface and is consistent with the proposed involvement of a weakly hydrated H_3O^+ as the initiator of oligomerization.¹²

Figures 2B, 3B, and 4B display the isotopic ratios RH^+/RD^+ measured in experiments on $\text{H}_2\text{O}/\text{D}_2\text{O}$ (50/50 = vol/vol) microjets as functions of pH. The contributions of the ^{13}C satellites of RH^+ signals to RD^+ signal intensities were subtracted in all cases. The RH^+/RD^+ values (i.e., the kinetic isotope effects, KIEs) for all products range between 2.0 and 3.5 and are independent of pH. These relatively small KIEs and their pH independence are in interesting contrast with those observed in the protonation of ISO under the similar condition.¹² We infer that the carbocations observed in the present study are longer-lived than those in the case of ISO and exchange their labels with the solvent prior to detection.^{27,28} RH^+/RD^+ ratios are deemed to reflect the lifetimes of their

precursors relative to the characteristic times for hydron exchange with the solvent.

Figures 5 and 6 show the plots of products signal intensities as functions of the mixing ratio of α -P(g), $[\alpha$ -P(g)], or β -P(g),

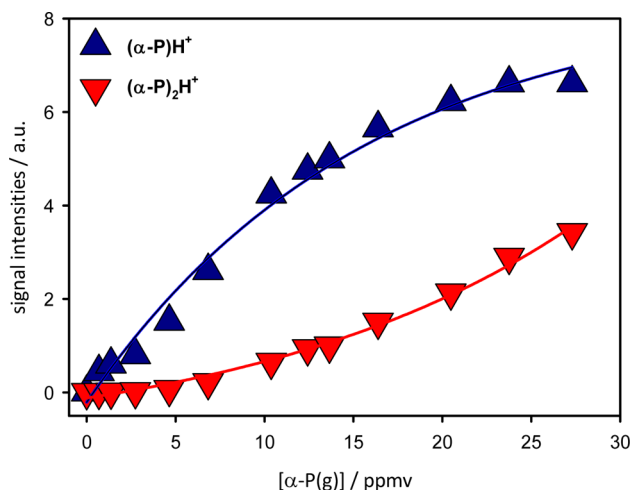


Figure 5. ES mass spectral signal intensities from aqueous microjets at pH 2.6 exposed to gaseous α -P(g) for ~ 10 – $50 \mu\text{s}$ contact times as a function of the α -P(g) mixing ratio; 1 ppmv = 2.4×10^{13} molecules cm^{-3} at 1 atm and 298 K experimental conditions.

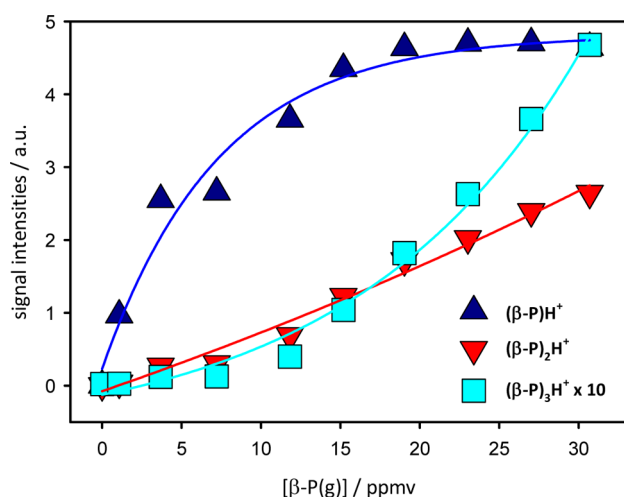


Figure 6. ES mass spectral signal intensities from aqueous microjets at pH 2.6 exposed to gaseous β -P(g) for ~ 10 – $50 \mu\text{s}$ contact times as a function of the β -P(g) mixing ratio. Note that the signal intensity of $(\beta\text{-P})_3\text{H}^+$ was multiplied by 10; 1 ppmv = 2.4×10^{13} molecules cm^{-3} at 1 atm and 298 K experimental conditions.

$[\beta\text{-P(g)}]$, respectively. Note the inverse curvatures and the nonvanishing initial slopes of $(\alpha\text{-P})\text{H}^+$ versus $(\alpha\text{-P})_2\text{H}^+$ curves and of $(\beta\text{-P})\text{H}^+$ versus $(\beta\text{-P})_2\text{H}^+$ and $(\beta\text{-P})_3\text{H}^+$ curves, as expected for a fast stepwise oligomerization process. The implication is that the initially protonated carbocation ($m/z = 137$) signals correspond to an intermediate produced in a rate-determining reaction at the gas–water interface, which is rapidly converted to the dimer and/or trimers. Accordingly, both $(\alpha\text{-P})\text{H}^+$ and $(\beta\text{-P})\text{H}^+$ signals approach a steady-state, whereas the dimer and trimer production accelerates at larger exposures. Very similar plots were obtained in the case of d -L. Taken together, these findings represent compelling evidence

that α -P(g), β -P(g), and d -L(g) undergo cationic oligomerization upon impact on mildly acidic water–air interfaces.¹⁸

It should be pointed out that reactant conversion is proportional to exposure, that is, $[\alpha\text{-P(g)}] \times \tau$ ($[\alpha\text{-P(g)}]$ is the mixing ratio; τ is contact time), rather than to the mixing ratio alone. Thus, the same ($10 \text{ ppmv} \times 10 \mu\text{s}$) exposures are realized by exposing water to 1 ppbv terpene(g) for 0.1 s or to 1 pptv terpene(g) for 100 s (1 ppbv = 2.4×10^{10} , 1 pptv = 2.4×10^7 molecules cm^{-3} under 1 atm and 298 K experimental conditions), if the surface of water is not saturated with terpenes at ppmv concentrations. A net reactive uptake coefficient for α -P in these experiments, $\gamma_{\alpha\text{-P}}$, may be evaluated from the expression for the number of reactive collisions per unit area during contact times, N , given by the kinetic theory of gases (eq E1)^{12,29}

$$N = \frac{1}{4} \gamma_{\alpha\text{-P}} \nu n_{\alpha\text{-P}} \tau \quad (\text{E1})$$

where $\nu = 2.15 \times 10^2 \text{ m s}^{-1}$ is the mean thermal speed of gaseous α -P at 298 K, $n_{\alpha\text{-P}}$ is number density, and $\tau \approx 10$ – $50 \mu\text{s}$ is the estimated gas–liquid contact time.¹⁸ By assuming that (1) the thickness of the interfacial liquid layer in which these processes take place is $\Delta \approx 5 \times 10^{-10} \text{ m}$ ¹⁸ and (2) the minimum detectable ion concentration ($\sim 0.5 \mu\text{M}$) in this setup is produced under ~ 20 ppbv (4.8×10^{11} molecules cm^{-3} at 1 atm, 298 K) mixing ratio, we estimate $\gamma_{\alpha\text{-P}} = 4.6 \times 10^{-5} < \gamma < 1.1 \times 10^{-3}$ for the reactive uptake of α -P on pristine (nonaged) water surfaces at $1 \leq \text{pH} \leq 3$ (Figure 2A). Estimated $\gamma_{\beta\text{-P}}$ and $\gamma_{d\text{-L}}$ fall in the same range. These values are >20 times higher than γ_{ISO} measured in the similar setup¹² and are in fair agreement with the reported uptake coefficient $\gamma = 1.2 \times 10^{-5}$ – 1.3×10^{-3} for pinonaldehyde, a product of the photooxidation of monoterpenes, on superacidic aerosols.³⁰ Our observation that $\gamma_{\alpha\text{-P}} > \gamma_{\text{ISO}}$ is qualitatively consistent with reports of the uptake of α -P(g) on acidic ($\text{pH} \approx -0.9$) aerosols versus the undetectable uptake of ISO(g) under the same conditions.¹⁷ The $\gamma_{\alpha\text{-P}} > 4.6 \times 10^{-5}$ value estimated from our experiments leads to surface resistances $R_C < 4/(\nu \gamma_{\alpha\text{-P}}) \approx 400 \text{ s m}^{-1}$ for the deposition of α -P(g) on mildly acidic surfaces. The product of $1/R_C$ times the surface-to-volume ratio ($S/V = 5 \text{ m}^{-1}$ of typical canopies (S/V is equivalent to the leaf area index, LAI, per meter of canopy column)³¹ yields a first-order rate constant for α -P deposition therein, $k_{\alpha\text{-P}} = (1/4)\gamma\nu(S/V) = 0.0125 \text{ s}^{-1}$, and half-lives of $\tau_{1/2} = 0.69/k_{\alpha\text{-P}} \approx 1 \text{ min}$ for α -P toward this process. According to these estimates, rates of dry deposition of terpenes are expected to be controlled (rate-determined) by their aerodynamic approach to foliar surfaces rather than by uptake itself.

Thus, significant reuptake of gaseous terpenes is expected to take place on the surfaces of leaves or soils that are only mildly acidic, say, $\text{pH} < 4$. It is also important to realize that only some plant species may emit ISO or terpenes, but they all supply viable sinks via this uptake mechanism.¹¹ This phenomenon seems not to be captured by emission rate measurements performed on single branches.³² Conventional measurements of the pH (the acidity) of the leaves' surfaces are necessarily indirect due to the need for rinsing and thereby diluting the small volumes of the relevant interfacial fluid films. However, there are several pieces of evidence suggesting that $\text{pH} < 4$ values should be prevalent. For example, fine aerosol particles consisting of NH_4HSO_4 incessantly settle on leaves and eventually deliquesce into films that ultimately reach $\text{pH} = -0.5$ in ambient air at 80% relative humidity.³³ Particles

containing oxalic acid would similarly approach $\text{pH} = 0.3$.³³ More to the point, the observation of significant emissions of HONO(g) ($\text{pK}_a = 2.9$) from forests³⁴ represents direct and compelling evidence that these ecosystems are indeed at $\text{pH} < 4$, for otherwise, HONO would be captured as NO_2^- and never escape into the air.

The preceding results and considerations therefore rationalize and support recent field studies, which concluded that the reactive uptake of gaseous terpenes by vegetation is more important than previously assumed by the atmospheric chemistry community.^{10,11} The fact that the bulk acidity required to drive cationic polymerization of gaseous terpenes on the surface of aqueous solutions is already attained at $\text{pH} < 4$ provides an unforeseen mechanism that should significantly enhance the yields of secondary organic aerosol from BVOCs predicted by current atmospheric chemistry models.^{35–37} Another interesting implication of the present study is the indirect biosyntheses of diterpenes ($\text{C}_{20}\text{H}_{32}$) and triterpenes ($\text{C}_{30}\text{H}_{48}$) from the deposition of monoterpenes on acidic surfaces. In this connection, it has been reported that ISO forms yellow/red-colored mono- and sesquiterpenes via dry deposition on 60–80 wt % sulfuric acid, which are released to the gas phase upon addition of water.³⁸ These “recycled” larger terpenes, presently observed as $(\text{monoterpene})_n$ ($n \geq 2$), may be re-emitted to the air³⁸ or, more likely, remain on the surface of leaves for further reaction with atmospheric oxidants. Further studies on this point are underway.

In summary, we found that gaseous α -P, β -P, and d -L are protonated and oligomerize on the surface of $\text{pH} < 4$ water. Our experiments demonstrate that the bulk acidity required to drive the cationic polymerization of gaseous olefins on the surface of aqueous solutions is already attained at $\text{pH} < 4$. The very similar titration curves of the products versus pH obtained from the three terpenes are compelling evidence that a barely hydrated hydronium ion, H_3O^+ , is present on the topmost layers of mildly acidic water, can transfer a proton to colliding terpene molecules, and thereby initiate an interfacial oligomerization process. The fact that only β -P produces trimers under the present conditions suggests that the differential nucleophilicities of exo (as in β -P) versus endo (as in α -P) or vinyl double bonds (as in d -L) modulate monomer reactivity and, hence, the extent of oligomerization.³⁹ More importantly, our findings provide a chemical uptake mechanism that operates in the environment at large, during day and nighttime, in the presence or absence of gas-phase oxidants, and may account for the efficient reuptake of BVOCs by the weakly acidic aqueous films lining the surfaces of leaves. By considering this universal uptake mechanism, it may be possible to narrow the gap between field observations and atmospheric model calculations.

■ EXPERIMENTAL SECTION

Gaseous terpenes are injected into a reaction chamber by sparging the liquid terpenes kept in traps held at 278 (α -P) or 288 K (β -P and d -L) in a temperature-controlled bath (THOMAS, TRC-4C) carried by ultrapure (>99.999%) nitrogen gas at known flow rates regulated by calibrated digital mass flow controllers (Horiba, STEC, SEC-400 MARK 3). We assume that the carrier gas is saturated with terpene vapors in each case. The Teflon gas lines were cleaned and dried by ultrapure nitrogen gas before/after measurements. The gas molecule hitting the surface of the pH -adjusted (by concentrated HCl; the pH was already measured by a calibrated pH meter, Horiba LAQUA F-74, before the experiments)

aqueous microjet (100 μm diameter) can stick to it by becoming protonated therein or rebound.^{28,29} The mixing ratios of terpenes in the reaction chamber are smaller than their vapor pressures^{40,41} by a dilution factor that can be calculated from the ratio of carrier and drying gas flow rates.

The carbocation products that we observe are formed when the gaseous terpenes collide with the intact electroneutral aqueous jets as they emerge from the nozzle, that is, before jets are broken up by the nebulizer gas. Because mass spectrometers detect net charge, the first step involves the separation of pre-existing anions from cations in the electroneutral jets. This is accomplished via the pneumatic breakup of the aqueous jet by a fast nebulizer gas that shears the outermost jet layers into droplets carrying net charges of either sign. Mass and charge separation is achieved by a high-speed annular $\text{N}_2(\text{g})$ jet that, by converting kinetic energy into surface and electrostatic energy, tears off the outermost layers of the nascent microjet into droplets carrying excess positive or negative charges that follow a normal distribution, as expected from a random fragmentation process.^{42–44} These net charges are proportional to the concentrations of the protonated terpenes and their oligomers produced during gas–liquid collisions. Because the nebulizer gas can fragment the jet but not the smaller droplets for hydrodynamic reasons, the creation of net charge is a one-time event. Note that collisions of gaseous terpenes with charged droplets within the spraying chamber do not affect their net charges. Charged droplets may hit the walls of the chamber, thereby being removed from the system. Thus, neither event will be registered in the mass spectra.

Also note that positively charged droplets contain a number of carbocations lacking balancing counterions, in numbers proportional to their concentrations in the interfacial layers of the microjet. Droplets subsequently evaporate solvent and become unstable due to charge crowding, whereby a cascade of Coulomb explosions produces increasingly smaller droplets. Unbalanced carbocations are ultimately ejected from the smallest droplets to the gas phase due to overwhelming electrostatic repulsion and become amenable to mass spectrometric detection. Notice that carbocations may recombine with remaining counterions (or associate with neutrals) in shrinking droplets, but the net current of unbalanced carbocations drawn per unit time from the microjet, that is, $j[(\alpha\text{-P})_n\text{H}^+]$ [ions \times time⁻¹], should be conserved in sprays of noninteracting droplets. $j[(\alpha\text{-P})_n\text{H}^+]$ should not be affected by ulterior collisions of (neutral) terpene with preformed droplets. As a result, mass spectral $(\alpha\text{-P})_n\text{H}^+$ signal intensities should be proportional to $j[(\alpha\text{-P})_n\text{H}^+]$ ($n > 1$) and, hence, to $j[(\alpha\text{-P})_n\text{H}^+(\text{if})]$, that is, they report the composition of interfacial layers at jet breakup. Further experimental details can be found in the SI or in our previous publications on the subject.^{15,18,45}

■ ASSOCIATED CONTENT

Supporting Information

Additional data and experimental details. This material is available free of charge via the Internet at <http://pubs.acs.org>.

■ AUTHOR INFORMATION

Corresponding Author

*E-mail: enami.shinichi.3r@kyoto-u.ac.jp (S.E.). ajcoluss@caltech.edu (A.J.C.).

Notes

The authors declare no competing financial interest.

■ ACKNOWLEDGMENTS

This work was supported by the Japan Science and Technology Agency (JST) PRESTO program and Grants-in-Aid from JSPS (Grant No. 23810013) and by NSF (U.S.A.) Grant AC-1238977. We are grateful to H. Mishra of Caltech for a helpful discussion.

■ REFERENCES

- (1) Pan, Y. D.; Birdsey, R. A.; Fang, J. Y.; Houghton, R.; Kauppi, P. E.; Kurz, W. A.; Phillips, O. L.; Shvidenko, A.; Lewis, S. L.; Canadell, J. G.; et al. A Large and Persistent Carbon Sink in the World's Forests. *Science* **2011**, *333*, 988–993.
- (2) Bouvier-Brown, N. C.; Goldstein, A. H.; Gilman, J. B.; Kuster, W. C.; de Gouw, J. A. In-Situ Ambient Quantification of Monoterpenes, Sesquiterpenes, and Related Oxygenated Compounds During Bearpex 2007: Implications for Gas- and Particle-Phase Chemistry. *Atmos. Chem. Phys.* **2009**, *9*, 5505–5518.
- (3) Camredon, M.; Hamilton, J. F.; Alam, M. S.; Wyche, K. P.; Carr, T.; White, I. R.; Monks, P. S.; Rickard, A. R.; Bloss, W. J. Distribution of Gaseous and Particulate Organic Composition During Dark α -Pinene Ozonolysis. *Atmos. Chem. Phys.* **2010**, *10*, 2893–2917.
- (4) Goldstein, A. H.; Galbally, I. E. Known and Unexplored Organic Constituents in the Earth's Atmosphere. *Environ. Sci. Technol.* **2007**, *41*, 1514–1521.
- (5) Carlton, A. G.; Wiedinmyer, C.; Kroll, J. H. A Review of Secondary Organic Aerosol (SOA) Formation from Isoprene. *Atmos. Chem. Phys.* **2009**, *9*, 4987–5005.
- (6) Seinfeld, J. H.; Pandis, S. N. *Atmospheric Chemistry and Physics: From Air Pollution to Climate Change*, 2nd ed.; Wiley: Hoboken, NJ, 2006.
- (7) Finlayson-Pitts, B. J.; Pitts, J. N. *Chemistry of the Upper and Lower Atmosphere*; Academic Press: San Diego, CA, 2000.
- (8) Ravishankara, A. R. Heterogeneous and Multiphase Chemistry in the Troposphere. *Science* **1997**, *276*, 1058–1065.
- (9) Enami, S.; Hoffmann, M. R.; Colussi, A. J. Prompt Formation of Organic Acids in Pulse Ozonation of Terpenes on Aqueous Surfaces. *J. Phys. Chem. Lett.* **2010**, *1*, 2374–2379.
- (10) Karl, T.; Harley, P.; Emmons, L.; Thornton, B.; Guenther, A.; Basu, C.; Turnipseed, A.; Jardine, K. Efficient Atmospheric Cleansing of Oxidized Organic Trace Gases by Vegetation. *Science* **2010**, *330*, 816–819.
- (11) Bamberger, I.; Hortnagl, L.; Ruuskanen, T. M.; Schnitzhofer, R.; Muller, M.; Graus, M.; Karl, T.; Wohlfahrt, G.; Hansel, A. Deposition Fluxes of Terpenes over Grassland. *J. Geophys. Res.* **2011**, DOI: 10.1029/2010jd015457.
- (12) Enami, S.; Mishra, H.; Hoffmann, M. R.; Colussi, A. J. Protonation and Oligomerization of Gaseous Isoprene on Mildly Acidic Surfaces: Implications for Atmospheric Chemistry. *J. Phys. Chem. A* **2012**, *116*, 6027–6032.
- (13) Donaldson, D. J.; Valsaraj, K. T. Adsorption and Reaction of Trace Gas-Phase Organic Compounds on Atmospheric Water Film Surfaces: A Critical Review. *Environ. Sci. Technol.* **2010**, *44*, 865–873.
- (14) Olah, G. A., Ed. *Superacid Chemistry*; Wiley: New York, 2009.
- (15) Enami, S.; Stewart, L. A.; Hoffmann, M. R.; Colussi, A. J. Superacid Chemistry on Mildly Acidic Water. *J. Phys. Chem. Lett.* **2010**, *1*, 3488–3493.
- (16) Blake, R. S.; Monks, P. S.; Ellis, A. M. Proton-Transfer Reaction Mass Spectrometry. *Chem. Rev.* **2009**, *109*, 861–896.
- (17) Liggio, J.; Li, S. M.; Brook, J. R.; Mihele, C. Direct Polymerization of Isoprene and α -Pinene on Acidic Aerosols. *Geophys. Res. Lett.* **2007**, DOI: 10.1029/2006gl028468.
- (18) Enami, S.; Hoffmann, M. R.; Colussi, A. J. Proton Availability at the Air/Water Interface. *J. Phys. Chem. Lett.* **2010**, *1*, 1599–1604.
- (19) Hunter, E. P. L.; Lias, S. G. Evaluated Gas Phase Basicities and Proton Affinities of Molecules: An Update. *J. Phys. Chem. Ref. Data* **1998**, *27*, 413–656.
- (20) Maleknia, S. D.; Bell, T. L.; Adams, M. A. PTR-MS Analysis of Reference and Plant-Emitted Volatile Organic Compounds. *Int. J. Mass Spectrom.* **2007**, *262*, 203–210.
- (21) Sigwalt, P.; Moreau, M. Reactivities of Carbocations and Monomers in Carbocationic Polymerization and Copolymerization. *J. Polym. Sci., Part A: Polym. Chem.* **2010**, *48*, 2666–2680.
- (22) Aoshima, S.; Kanaoka, S. A Renaissance in Living Cationic Polymerization. *Chem. Rev.* **2009**, *109*, 5245–5287.
- (23) Kostjuk, S. V.; Ganachaud, F. Cationic Polymerization of Vinyl Monomers in Aqueous Media: From Monofunctional Oligomers to Long-Lived Polymer Chains. *Acc. Chem. Res.* **2010**, *43*, 357–367.
- (24) Enami, S.; Hoffmann, M. R.; Colussi, A. J. Simultaneous Detection of Cysteine Sulfenates, Sulfinate, and Sulfonate During Cysteine Interfacial Ozonolysis. *J. Phys. Chem. B* **2009**, *113*, 9356–9358.
- (25) Enami, S.; Hoffmann, M. R.; Colussi, A. J. Absorption of Inhaled NO₂. *J. Phys. Chem. B* **2009**, *113*, 7977–7981.
- (26) Mishra, H.; Enami, S.; Nielsen, R. J.; Hoffmann, M. R.; Goddard, W. A.; Colussi, A. J. Anions Dramatically Enhance Proton Transfer through Water Interfaces. *Proc. Natl. Acad. Sci. U.S.A.* **2012**, *109*, 10228–10232.
- (27) Brastad, S. M.; Albert, D. R.; Huang, M. W.; Nathanson, G. M. Collisions of DCl with a Solution Covered with Hydrophobic and Hydrophilic Ions: Tetrahexylammonium Bromide in Glycerol. *J. Phys. Chem. A* **2009**, *113*, 7422–7430.
- (28) Dempsey, L. P.; Brastad, S. M.; Nathanson, G. M. Interfacial Acid Dissociation and Proton Exchange Following Collisions of DCl with Salty Glycerol and Salty Water. *J. Phys. Chem. Lett.* **2011**, *2*, 622–627.
- (29) Davidovits, P.; Kolb, C. E.; Williams, L. R.; Jayne, J. T.; Worsnop, D. R. Mass Accommodation and Chemical Reactions at Gas–Liquid Interfaces. *Chem. Rev.* **2006**, *106*, 1323–1354.
- (30) Liggio, J.; Li, S. M. Reactive Uptake of Pinonaldehyde on Acidic Aerosols. *J. Geophys. Res.* **2006**, *111*, D24303.
- (31) Makar, P. A.; Fuentes, J. D.; Wang, D.; Staebler, R. M.; Wiebe, H. A. Chemical Processing of Biogenic Hydrocarbons within and above a Temperate Deciduous Forest. *J. Geophys. Res.* **1999**, *104*, 3581–3603.
- (32) Guenther, A.; Karl, T.; Harley, P.; Wiedinmyer, C.; Palmer, P. I.; Geron, C. Estimates of Global Terrestrial Isoprene Emissions Using MEGAN (Model of Emissions of Gases and Aerosols from Nature). *Atmos. Chem. Phys.* **2006**, *6*, 3181–3210.
- (33) Clegg, S. L.; Brimblecombe, P.; Wexler, A. S., Eds. <http://www.aim.env.uea.ac.uk/aim/aim.php> (2011).
- (34) Sorgel, M.; Trebs, I.; Serafimovich, A.; Moravek, A.; Held, A.; Zetzsch, C. Simultaneous HONO Measurements in and above a Forest Canopy: Influence of Turbulent Exchange on Mixing Ratio Differences. *Atmos. Chem. Phys.* **2011**, *11*, 841–855.
- (35) Kalberer, M.; Sax, M.; Samburova, V. Molecular Size Evolution of Oligomers in Organic Aerosols Collected in Urban Atmospheres and Generated in a Smog Chamber. *Environ. Sci. Technol.* **2006**, *40*, 5917–5922.
- (36) Kalberer, M.; Paulsen, D.; Sax, M.; Steinbacher, M.; Dommen, J.; Prevot, A. S. H.; Fisseha, R.; Weingartner, E.; Frankevich, V.; Zenobi, R.; et al. Identification of Polymers as Major Components of Atmospheric Organic Aerosols. *Science* **2004**, *303*, 1659–1662.
- (37) Virtanen, A.; Joutsensaari, J.; Koop, T.; Kannosto, J.; Yli-Pirila, P.; Leskinen, J.; Makela, J. M.; Holopainen, J. K.; Poschl, U.; Kulmala, M.; et al. An Amorphous Solid State of Biogenic Secondary Organic Aerosol Particles. *Nature* **2010**, *467*, 824–827.
- (38) Connelly, B. M.; Tolbert, M. A. Reaction of Isoprene on Thin Sulfuric Acid Films: Kinetics, Uptake, and Product Analysis. *Environ. Sci. Technol.* **2010**, *44*, 4603–4608.
- (39) Anslyn, E. V.; Dougherty, D. A. *Modern Physical Organic Chemistry*; University Science Books: Sausalito, CA, 2006.

- (40) Hawkins, J. E.; Armstrong, G. T. Physical and Thermodynamic Properties of Terpenes. 3. The Vapor Pressures of α -Pinene and β -Pinene. *J. Am. Chem. Soc.* **1954**, *76*, 3756–3758.
- (41) Yaws, C. L. Chemical Properties Handbook: Physical, Thermodynamics, Environmental Transport, Safety & Health Related Properties for Organic & Inorganic Chemicals; McGraw Hill: New York, 1999.
- (42) Dodd, E. E. The Statistics of Liquid Spray and Dust Electrification by the Hopper and Laby Method. *J. Appl. Phys.* **1953**, *24*, 73–80.
- (43) Theofanous, T. G.; Mitkin, V. V.; Ng, C. L.; Chang, C. H.; Deng, X.; Sushchikh, S. The Physics of Aerobreakup. II. Viscous Liquids. *Phys. Fluids* **2012**, DOI: 10.1063/1061.3680867.
- (44) Zilch, L. W.; Maze, J. T.; Smith, J. W.; Ewing, G. E.; Jarrold, M. F. Charge Separation in the Aerodynamic Breakup of Micrometer-Sized Water Droplets. *J. Phys. Chem. A* **2008**, *112*, 13352–13363.
- (45) Enami, S.; Hoffmann, M. R.; Colussi, A. J. Molecular Control of Reactive Gas Uptake “On Water”. *J. Phys. Chem. A* **2010**, *114*, 5817–5822.